

## RHEOLOGICAL ISSUES IN THE PAPER INDUSTRY

**Douglas W. Bousfield**

University of Maine  
Orono, ME 04469-5737 USA  
bousfld@maine.edu

### **ABSTRACT**

The paper industry has a number of processes where the rheology is complex and critical to control for trouble free operation. The rheological properties of pulp suspensions and paper coatings are reviewed here. The flow, rheology and other various phenomena are discussed for pulp suspensions. The particle level models that have been developed for pulp suspensions are compared to experimental results. Paper coating suspension rheology and the coating flow fields are described. Particle level models are discussed and compared to various rheological properties and process issues. Some open questions are identified.

**KEYWORDS:** Suspension rheology; pulp rheology; coating rheology; Stokesian Dynamics; viscoelasticity; yield stress

---

## 1. INTRODUCTION

The pulp and paper industry is a significant part of many developed economies. Paper products play a role in a number of aspects of our society such as packaging, hygiene, and communication. Many paper products are recycled and will play a role in the future. The flow behavior of a number of process streams is important to this industry and for processing of the final product during converting operations. An early review of this topic related to the paper industry was given in 1960 with a focus on fiber suspensions, wet webs, and paper deformation in the converting operations [1]. This review will focus on the state of knowledge of the flow properties of paper fiber suspensions and pigmented paper coatings.

The flow behavior of various process streams is critical to the design and trouble-free operation of the typical paper mill. Casey is a standard reference text that describes all areas of the paper industry [2]. For many mills, wood chips are a raw material that must be screened and transported to the digester; many details with regard to chip moisture content and size determines the ability of the chips to move in channels and hoppers. In kraft pulp mills, chips are mixed with chemicals to break down the wood to fibers. This mixture must flow from the reactor and is washed in a series of filtration steps to separate out the fibers from the spent chemicals. The fibers are often “bleached” to make them white before dilution and distribution to a paper machine. Transporting these fiber suspensions from various processes at high solids content requires careful design of equipment and experience related to the flow properties of these suspensions. The fibers are often “refined” or “beaten” to modify the fiber properties. The headbox of the paper machine distributes fibers across the width of the paper machine: the fiber suspension needs to flow in a uniform manner at high velocities, keeping the fibers from flocculation, through a narrow gap. The width of a modern paper machine can be several meters. The fiber suspension drains in one or two directions through a fine wire to form a wet mat that is pressed and dried to produce paper.

The recovery cycle in a kraft mill has a number of difficult process streams. The spent chemicals from the process are concentrated to a high solids solution through multiple effect evaporation. This solution is sprayed into a recovery boiler to burn the organic phase and to recover the chemicals; the flow properties of this solution is critical to obtain good spray characteristics. The chemicals are reactivated through a few processes linked to a lime cycle.

The flow properties of coatings, sizings, inks, and other surface treatments are important for down-stream processing of the product for various grades. Coatings are often applied to paper with rolls or blades and must have good rheology at high shear rates. Inks are often high viscosity fluids that can generate significant forces to the paper surface during printing; if these forces are too high, coating or fibers can be “picked” from the surface to generate defects. Starch solutions are often used to modify the paper properties. These solutions must be at the correct viscosity in the equipment used to apply them. The deformation behavior of the final product, its stiffness, tensile strength, and response to humidity are also rheological topics that are critical to the final product properties [1].

Even though rheology of a number of process streams is important to the industry, only two have received a significant attention in the literature: 1) pulp suspensions composed of wood fibers in water and 2) paper coatings that often consist of pigments, latex binders, and other additives in water. This review will focus on these two suspensions because of their general importance to the industry.

## 2. PULP SUSPENSIONS

The characteristic rheology of pulp suspensions depends on a number of parameters such as concentration, fiber properties, and the presence of other components such as fillers, retention aids, defoamers and anti-microbial agents. The two major types of pulps are 1) mechanical pulps, obtained from mechanically grinding wood and used for products such as newspaper, and 2) chemical pulps that are obtained from a chemical breakdown of the wood with the kraft or sulphite process. Some fibers are released in other various methods such as thermo-mechanical pulps (TMP). Standard texts and handbooks describe these processes in detail [2]. Mechanical pulps tend to have short fibers while chemical pulps can have longer fibers that are typically 20-40  $\mu\text{m}$  in diameter and 1-5 mm in length. The potential for the fibers to form networks that help transmit stresses cause these suspensions to have behavior that are quite different from other solid particle suspensions. Non-Newtonian behavior is seen often for fiber concentrations as low as 0.5% by weight. Cui and Grace provide a recent general review of the literature with regard to the flow and behavior of pulp fiber suspensions [3].

### 2.1. Pipe flow of pulp suspensions

The pressure loss in pipes and fitting for the flow of pulps has been of interest since the 1950s. Even suspensions at 1% by weight solids had a significantly different flow behavior than water, and this difference was not systematic for all fiber types. At low flow rates, the pressure losses were much larger than water. As the mean flow velocity increased, the pressure losses relative to water decreased. In the turbulent region, the fibers acted as a drag reducer and generate a lower pressure loss than water. Figure 1 illustrates the typical behavior (after Moller [4]).

A number of early reports correlate the pressure loss in the empirical form

$$\frac{\Delta H}{L} = KV^\alpha C^\beta D^\gamma \quad (1)$$

where  $\Delta H/L$  is the pressure head loss,  $V$  is velocity,  $C$  is consistency, and  $D$  is the internal pipe diameter, and  $K$ ,  $\alpha$ ,  $\beta$ ,  $\gamma$  are constants [5]. These constants depend on the pulp type and the pipe roughness and are given in methods published by the Technical Association of the Pulp and Paper Industry (TAPPI) such as TIS 408-4. If these results are expressed in terms of friction factor and Reynolds number, each concentration of fiber and fiber type has a different curve [5].

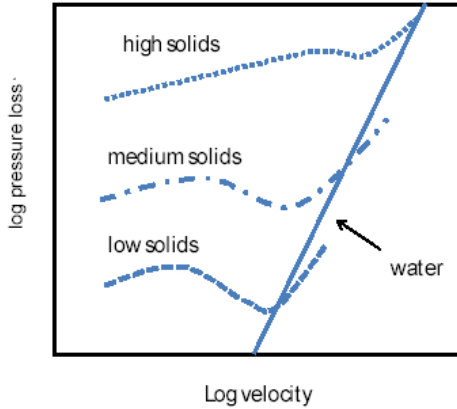


**Figure 1:** Typical pressure gradients measured for pulp suspensions compared to water. Low to high solids curves represent results that range from 0.5 to 4% solids resembling those in Ref. [4].

Using a friction factor type format, data for different consistencies can be collapsed onto a single curve, but chemical pulps had a different correlation than mechanical pulps. Wall roughness had some influence also on the data. Figure 2 shows the general trend of the data for chemical pulps and the range, for a modified friction factor and Reynolds number based on the wall shear stress defined as

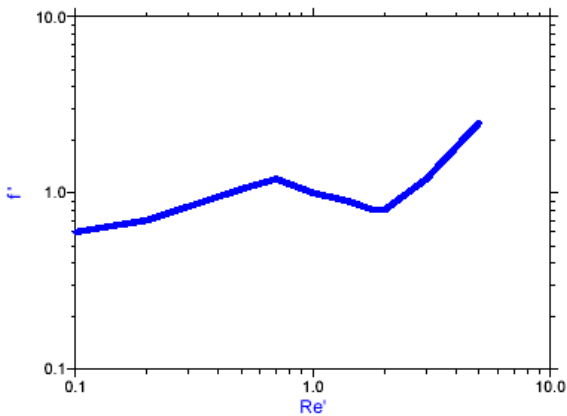


**Figure 2:** Typical correlation for chemical pulps for the modified friction factor and Reynolds number.

$$f' = \frac{\Delta P D}{4\tau_D L} \quad (2a)$$

$$\text{Re}' = \left( \frac{V^5 \rho^2 \mu}{\tau_D^3 D} \right)^{1/6} \quad (2b)$$

where  $\Delta P/L$  is the pressure loss for a length of pipe,  $\rho$  is density,  $\mu$  is the viscosity of water, and  $\tau_D$  is a wall shear stress or yield stress for the fiber network that depends on consistency and the type of fibers. Typical correlations for this stress are found in Moller and Elmqvist [6]: values range from 5 to 200 N/m<sup>2</sup> as consistencies go from 1 to 5%, respectively. To use this correlation, the yield stress for the network is obtained from data or correlations for fibers of that type and different concentrations. This yield stress is used to calculate a modified Reynolds number in Eq. (2b) for a desired average velocity. A friction factor is obtained, from Fig. 2. Finally, a pressure loss can be calculated from Eq. (2a).

The decrease in friction factor near the value of one for this modified Reynolds number correlates with the turbulence drag reduction that occurs with these suspensions. At low concentrations of fibers, less than 1%, pressure loss correlations follow that of a Newtonian fluid if the viscosity of the suspension is used [7]; this indicates that some of the correlation in Eq. (2) may be improved by using the viscosity of the suspension. Others give methods for the optimum design of pipelines for pulps [8-10].

The pressure loss in fittings and valves is found to scale with the water case [7]. For gate vales, elbows, expansions and contractions, the ratio of the loss factor to that of water was between 1.3 and 2.5 for 3% concentration of fibers. TMP fibers had lower loss factors.

## 2.2. Rheology of pulp suspensions

A review of the literature that focuses on the rheology of pulp suspensions is given by Kroeher [11]. If the results, displayed in Figure 1, are expressed in terms of shear stress, two critical stresses are helpful to characterize the system, as depicted in Figure 3. At low shear rates, the stress needed to overcome the network stress of the suspension needed to cause some initial flow; this stress is called a yield stress  $\tau_Y$ , even though this may not be a “true” yield stress. At higher flow rates, another critical stress is needed to fully disrupt the system to obtain turbulent flow,  $\tau_D$ . The mechanism behind the flow behavior relates to the formation of a water layer near the pipe surface shown in Figure 4 [12]. As velocity increases, most of the suspension moves as a plug and is lubricated by a water layer between the wall and the plug. This behavior has been seen with other suspensions that develop a wall slip phenomena. At higher velocities, the annulus layer becomes turbulent and the plug layer decreases. At high velocities, the plug layer becomes turbulent, but the presence of fibers gives some amount of drag reduction. This slip layer and plug flow nature of the pulp flows were directly imaged using Nuclear Magnetic Resonance (NMR) [13]: softwood pulps had

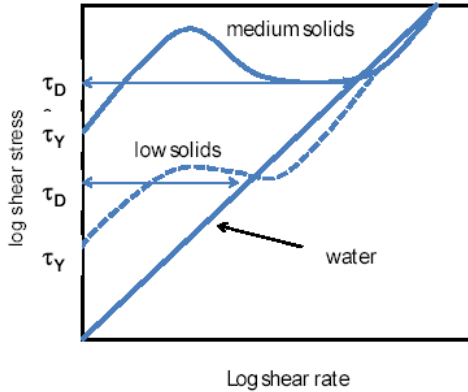


**Figure 3:** Shear stress-shear rate data for pulp suspensions showing yield and disruptive stress values.

extreme plug flow behavior while hard wood pulps had moderate plug flow type behavior at 0.86 wt% concentration. Optical probes were also used to measure boundary layer thicknesses in pulp flows that linked the pressure drop in the pipe to lubricated plug flow and a transition to turbulent flow [14]. Pitot tube measurements also indicate a plug motion of the suspension [15].

If the results of rheological tests shown in Figure 3 are expressed in terms of shear stress and shear rate, the behavior follows the Herschel-Bulkley model in a limited shear rate range as

$$\tau = \tau_Y + K(\dot{\gamma})^n \quad (3)$$

where  $\tau$  is shear stress,  $\tau_Y$  is a yield stress and  $K$  and  $n$  are parameters. If the applied stress is less than the yield stress, no flow occurs. The yield stress of pulp suspensions

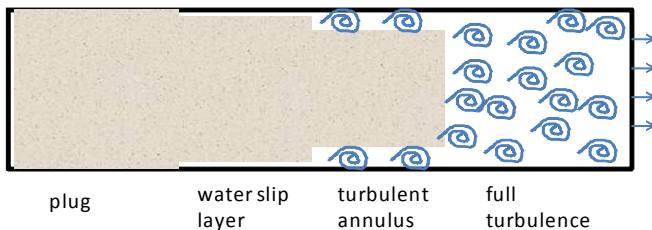


**Figure 4:** Various flow regions as velocity increases, from Ref. [12].

has been of high interest because of the importance in several difference processes. The influence of fiber length, concentration and temperature on the yield stress and other parameters was recently reported by Ventura *et al.* [15].

The yield stress of a pulp suspension becomes an important parameter to understand and characterize and has been the subject of a number of reports [16-23]. The yield stress was found to depend on fiber concentration and air content as

$$\tau_y = aC^b(1-\phi)^c \quad (4)$$

where  $C$  is the concentration expressed as a weight percentage,  $\phi$  is the volume fraction of air in the suspension, and  $a$ ,  $b$  and  $c$  are parameters [17]. This yield stress should be measured in devices with vanes or baffles to prevent the slippage of the water layer. Kerekes *et al.* report values for the parameter  $a$  between 1.8 and 25 and  $b$  between 1.7 and 3.0 [18]. Others report values of the coefficient  $a$  ranging from  $1.3 \times 10^6$  to  $1.4 \times 10^7$  when  $C$  is expressed as a mass fraction instead of a percentage; the parameter “ $b$ ” was in the range of 2.7 to 3.7. The parameter “ $c$ ” ranged from 2.2 to 3.3. The value of the coefficient  $a$  is known to be a function of the fiber length and has been found to scale with the length squared [19]. A fiber network theory predicts  $b=3$  [20].

The shear stress to disrupt the plug may be different than the yield stress for initial flow. If the conditions are used at the point of drag reduction, this plug disruptive stress should also take the form of Eq. (4) and is reported to be in the order of 50-300 Pa [21]. Correlations for this stress are given in Venura *et al.* [15]. An analysis of the drag reduction regime is given in Lee and Duffy [20]. A shear factor has also been introduced to characterize pulp suspension flow in small channels and refiners [24].

Pulp suspensions have been found to have significant viscoelastic properties [25-28]. This behavior is not surprising in view of the network structure that naturally forms; this network structure can store energy during deformation. The influence of various additives, such as cationic polymer, on these properties has been reported.

### 2.3. Floc disruption

Of equal importance to the flow properties of pulp suspensions is the uniformity of fiber distribution as the suspension is drained on the wire of the paper machine. Flexible fiber suspensions often flocculate and form heterogeneous structures called “flocs”, even at solids less than 1%. The shear forces needed to disrupt these flocs is important to understand for proper design of headboxes. Studies suggest that flocs are held together by elastic fiber interlocking [23]. For stagnant situations, the formation of flocs has been reported to correlate with a crowding number

$$N_c = \frac{C_m L_f^2}{2\omega} \quad (5)$$

where  $C_m$  is the concentration of fibers in mass per unit volume,  $L_f$  is the length-weighted fiber length average, and  $\omega$  is the fiber coarseness defined as the mass per unit length of fiber [23]. When this crowding number is larger than 16, fibers interact and the fiber mobility is limited. For a flowing situation, the dimensionless group that correlates the results is

$$\varepsilon = \frac{\tau_y}{\rho U^2} \quad (6)$$

where the same yield stress described above is made dimensionless with the turbulent stresses of the flow field, where  $\rho$  and  $U$  are the density and characteristic velocity of flow, respectively. When this group is less than  $10^{-2}$ , then uniform formation is observed; the flow field is able to disrupt flocs [29].

#### 2.4. Particle level models of fiber suspensions

A number of models have been proposed to predict the rheology of fiber suspensions. Batchelor [30,31] proposed expressions to describe the stress in a suspension of rigid semi-dilute rigid fibers; slender body theory was used to calculate the stress contribution from particle-fluid interactions. The viscosity scaling parameter of  $nL^3$  comes from this analysis, where  $n$  is the number of fibers per unit volume and  $L$  is a fiber length scale.

Particle level models have been demonstrated to be able to link small-scale phenomena such as colloidal forces to macroscopic scale behavior such as viscosity. Much work has been reported for spheres suspended in a Newtonian fluid, but less for fibers. Claeys and Brady [32,33] described fibers as rigid prolate spheroids and developed expressions to describe long range and fiber-fiber interactions. Others used approximate hydrodynamic interactions between rigid fibers to predict suspension viscosity; good results were obtained for  $nL^3 < 50$  [34-35]. Others have used slender rigid rods that interact only through contact forces [36,37]. As concentration increased, the behavior is dominated by fiber contacts. These simulations do not report shear thinning nor floc development.

Flexible fibers have been modeled with several methods. Yamamoto and Matsuoka described fibers as chains of rigid spheres connected through springs [38]. Ross and Klingenberg modeled flexible fibers as chains of prolate spheroids connected through joints [39]. This method was extended by using spherocylinders connected by joints; fibers equilibrium shape, flexibility, and interfiber friction were found to be important [40]. Switzer and Klingenberg demonstrated that fiber shape and friction are the key parameters in terms of the predicted viscosity [41]. Viscosity was predicted to scale as  $nL^3$ , but at different slopes depending on shape and the friction coefficient. Flexibility of the fibers did not influence viscosity, but it did influence floc formation. The yield stress was found to scale with the form of Eq. (4), with  $b = 2.8$ ; the value of  $a$  did not match experiments, but details of the some of the experimental parameters were not known. The results do predict a shear thinning behavior often seen. Recent work by Lindstrom and Uesaka [42-43] predict fibers shapes in simple shear that seem

quite realistic. Including several fibers and fiber interactions, viscosities are predicted that compare well with experimental data. Again, fiber friction is found to be an important parameter. Normal forces are also predicted with this model that compares well with experiments. In view of the complexity of this system, these models show excellent ability to predict behavior and help illustrate mechanisms that lead to various flow behaviors.

The general behavior of fiber depletion at the walls of the pipe has not been studied with particle level models. However, the potential is clear to take models as above and include wall effects. In addition, particle level models may be able to predict viscoelastic properties.

## **2.5. Models of pulp suspension flows**

For dilute suspensions that correspond to headbox flows and the final drainage of the suspension, good predictions have been reported assuming a Newtonian fluid, as long as the buildup of a fiber mat on the boundary is taken into account. For flow in the headbox, turbulent models are expected to be needed to capture the physics. The uniformity of flow at the exit and the level of turbulence are critical issues. A recent example of the prediction of turbulence and fiber orientation in a converging flow is given by Olson et al. [44].

A number of models have been reported to predict the pressure pulses and dewatering of pulps suspensions for twin wire forming machines [45-47]. In this geometry, the pulp suspensions is trapped between to permeable flexible wires. These wires deform around rolls or blades. The deformation of the wire generates pressure gradients in the suspension and causes some amount of water to flow through the wires. These pressure pulses cause machine direction flows for short time periods that help improve the uniformity of the final sheet. These machines are designed based on simple models that predict dewatering. These models often neglect viscosity because inertial effects dominate.

## **3. PAPER COATINGS**

Paper and paperboard are often coated to improve the appearance of the sheet and the quality of the print of the final product. Products such as magazines, catalogs, labels, and consumer packaging are often coated. For example, a coating is applied to recycled fibers to cover the grey or brown appearance to produce the common box in food packaging. The coating is normally composed of a pigment such as kaolin or calcium carbonate, a latex binder, and a soluble binder such as starch. Coatings are formulated at high solids content in order to minimize drying requirements and to improve quality. The coating must be mixed, pumped, re-circulated, and metered onto the moving paper web. The final metering or coating operation is the critical step in the process; the coated layer must be free from defects and near a target coat weight. The rheology of the coating is an important issue in the control, design, and operation

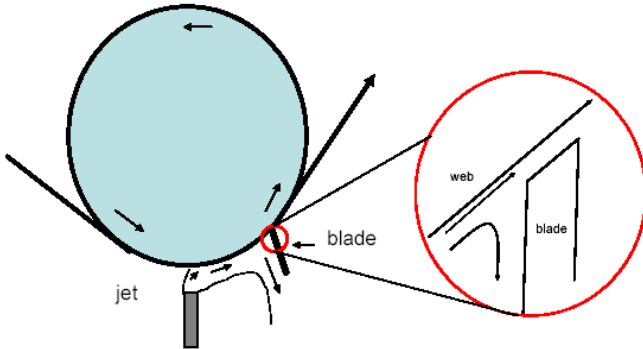


**Figure 5:** Schematic of a jet applicator-blade metering system. The right hand side of the figure is an enlargement of the blade region.

of the coating process. A comprehensive description of the materials and processes is given by Walters [48]. A review of paper coating rheology was given by Bousfield and Co [49]. There is a common trade-off between high solids to minimize drying costs and improve quality and low solids to promote good rheology and trouble free operation [50].

Most coating methods apply an excess of coating to the paper web and the final coat weight is controlled by a steel blade or air jet. The steel blade is the most common method for publication grades [48]. The excess of coating is applied with roll applicators, a pressurized pond in front of the blade, or a jet; a jet applicator system is depicted in Figure 5. In the piping system, the shear rates are moderate. The web speed is often 15-20 m/s and the gap between the blade and the web is on the order of 20  $\mu\text{m}$ . Therefore, the shear rate under the blade is on the order of  $10^6 \text{ s}^{-1}$ . The thickness of the blade is around 0.5 mm [48]. The time an element of fluid spends in the high shear rate region is less than 1 ms. Therefore, the coating must be able to respond to this rapid acceleration and high shear rate. The details of the blade geometry are shown in the right hand side of Figure 5. High solids content leads to high blade forces that can cause web breaks or scratches.

One other established method and two methods in development are based on pre-metering the coating before application. The metered size press uses rods working against a rubber backing roll to apply a film of coating onto the roll; this film is pressed against the paper in a nip. Curtain coating and spray coating are common in other industries, but have limited application in the paper industry. Both of these methods control the coat weight before the coating reaches the paper.

There are a number of unique aspects of paper coating that make this operation complex. The web is rough, porous, and absorbent. In addition, it changes its physical properties upon contact with water. The final coating layer thickness ranges from 7 – 30  $\mu\text{m}$ . The web is compressible, along with the rubber backing that supports the blade

loading. The blade is slightly flexible and is mounted and loaded in various ways. Steel blades wear during operation and are changed on a regular basis. All of these factors, including the high speeds, cause paper coating to be a complex operation.

The operational difficulties or “runnability” problems vary widely in the industry, but common problems are the scratches, streaks, or skips in the coating layer and the buildup of coating on the blade. The buildup on the blade in itself is not a problem, but when the buildup breaks off the blade and ends up on the web, problems in the calendering and printing operations develop. The blade buildups are often called “whiskers”, “stalagmites”, “weeps”, or “spits”, depending on the operator and the nature of the building (dry or wet). Other operational problems are related to coat weight control, both in the machine and cross-machine directions. Another common problem is web breaks; these cause a loss of production and correlate to high blade forces. Many of these problems are related to rheology of the coating.

Rotating spindle devices are a common method to measure the viscosity of a coating in the industry. These are low shear rate tests that record the viscosity at certain shear rates. Control is often determined looking at just one shear rate. A concentric cylinder test is common to obtain the high shear rate behavior. Shear rates in the order of  $10^5 \text{ s}^{-1}$  can be obtained. Capillary viscometers have been used to characterize the results at shear rates over one million [48].

The viscosity measurement in steady-state shear flow is an important predictive tool. Examples of works are Carreau and Lavoie [51], Purkayastha and Oja [52], and Ghosh [53]. To obtain the viscosity function over a wide range of shear rates, one usually has to utilize several viscometers: the cone-and-plate system for low shear rates, the concentric cylinders configuration for medium to high shear rates, and the

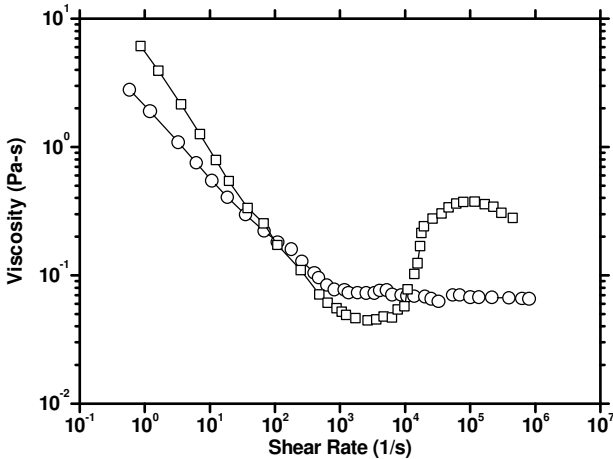


**Figure 6:** The viscosity functions of a starch-containing coating (open circle) and a coating with latex particles (open square). Data are from Roper and Attal [55].

capillary type for high shear rates. The general results are typical of any suspension. One concern with steady tests is that they do not characterize the dynamic response that may be important in the coating operation.

The behavior of the viscosity versus shear rate curve depends on the pigment concentration, pigment particle size distribution, the latex level and particle size, and the presence of soluble binders or thickeners. The rheology is typical of high solids suspensions [54]. Figure 6 is an example of the viscosity curves of a starch-containing formulation and a formulation with latex particles (from Roper and Attal [55]). The curve of the starch-containing formulation exhibits a power-law shear-thinning region and a region of almost constant viscosity at high shear rates. On the other hand, the formulation with latex particles shows a region with shear-thickening or dilatant behavior. Beyond the power-law shear-thinning region, the viscosity rises sharply with increasing shear rate and then decreases slightly at higher shear rates. Roper and Attal [55] indicated that the dilatant behavior depended on the solids level and the latex particle size; the extent of dilatant behavior was increased with higher solid levels and larger latex particle size. The onset of shear thickening in suspensions has been reviewed by Barnes et al. [54]. Quantitative predictions of the onset of shear thickening is still lacking.

Aside from the solid levels and the size and shape of solid particles, the polymer additives dissolved in the suspending medium also have considerable effects on the rheological behavior of the coating suspension as expected. One example is shown in Figure 7, which depicts the viscosity curves for a polymeric thickener added into the suspension. Common thickeners are carboxy methyl cellulose (CMC), and other synthetic polymers based on acrylic or urethane chemistries. Especially with thickeners like CMC, the increase in suspension viscosity is much larger than the increase in the viscosity of the liquid phase. This result indicates that the polymer induces some interaction between particles.

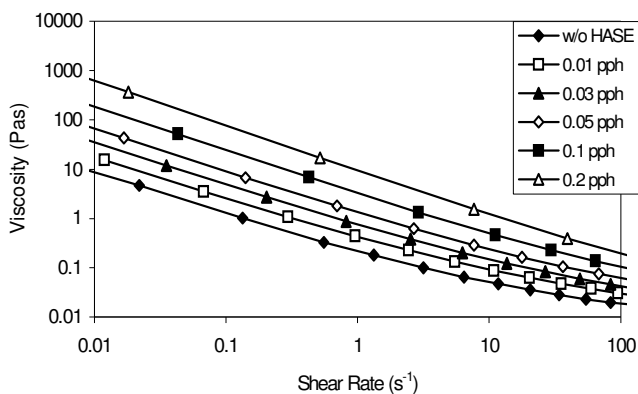


**Figure 7:** Effect of a polymeric thickener on the steady shear viscosity of a typical coating formulation, from Nisogi and Bousfield [56].

The storage modulus of these coatings is often found to be larger than the loss modulus. This result indicates a significant elastic effect. Windle and Beazley [57] suggested that viscoelastic effects would influence blade forces. The discussion on viscoelastic properties was focussed on the extra normal forces generated during shear: these normal forces could contribute to the hydrodynamic lift forces during operation. An expression for the extra force on the blade due to normal forces was proposed. Triantafillopolous [58] gives an extensive review of the viscoelastic nature of coatings and the implication in coating processes. One key question is that while small amplitude oscillatory flows have significant elastic behavior, large scale flows, such as the exit of a capillary, do not show the die swell associated with elastic fluids. The elastic structure must be broken down with strain and disrupt the interactions that give rise to the elastic behavior. This break down in structure is seen by the increase in storage modulus as a function of time after steady shear [56].

Figure 8 shows the linear viscoelastic data of Fadat and Rigdahl [59] for a clay-based coating color with a different grade of CMC. Here the behavior of the storage modulus is more like that of a viscoelastic liquid. The reduction of the phase angle with increasing frequencies indicates that the suspensions becomes more solid-like at higher frequencies.

Transient shear-flow experiments have been used to elucidate the characteristic times of structure formation or breakup in coating suspensions. A common industrial practice is to generate a hysteresis loop from shear stress measurements completed over a strain-rate sweep for a finite time interval. The stress growth measurement upon the inception of steady shear flow, as described by Ghosh [53] is an example of a test that gives transient information with finite strain. These experiments were able to yield estimated characteristic times of the coating suspensions studied.

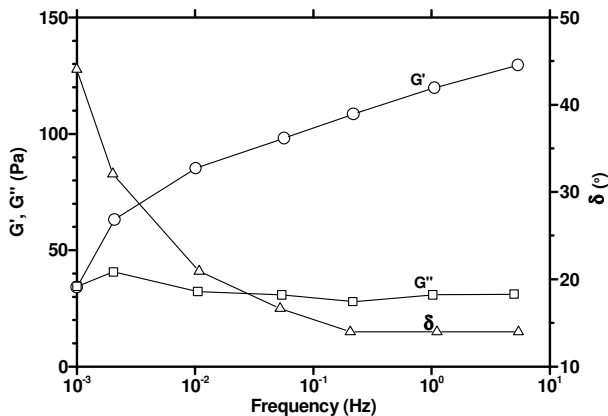


**Figure 8:** The dependence of the storage and loss moduli and phase angle on the frequency for a clay-based coating color containing 1.25 part of CMC per 100 parts of clay. Data are from Fadat and Rigdahl [59].

Just like with pulp suspensions, at some conditions, there seems to be evidence of a slip layer that lubricates the flow near boundaries [60]. The conditions that cause this slip have not been well characterized and the prevalence in industrial processes is not clear.

Due to the converging-diverging geometry in the coating operation, the flow is both shearing and extensional. In the metered size press process, the exit of the nip has high extensional flows. Therefore, extensional viscosity may therefore play a significant role. Various methods have been attempted to characterize the extensional viscosity [61-63].

### **3.1. Particle level models**

In the blade coating process, the gap between the blade and the paper web can be on the order of 15  $\mu\text{m}$ . In addition, high points of the paper may generate even smaller gaps. Most of the pigments are less than 2  $\mu\text{m}$  in diameter, but some high aspect ratio pigments may have dimension on the order of 10  $\mu\text{m}$  or more. Therefore, the dimension of the gap is on the same order of magnitude as the pigments. Particle level descriptions of these flows become important, especially in view of the difficult experimental situation that exists with high speeds, thin opaque layers, and micron scale particles. The goal of particle level modeling work is to help explain large scale phenomena based on fine scale interactions.

Particle level models were introduced by Brady and Bossis [64,65] to relate the microscopic behavior of suspension to their macroscopic behavior such as rheology. Stokesian dynamics is a technique to calculate the trajectories of particles in a suspension undergoing flow. The technique has been shown to predict various phenomena. These include the increase of viscosity with increasing solids described by Durlofsky et al. [66] and Toivakka and Eklund [67], the reduction of the viscosity of a mixture of large and small spheres given by Chang and Powell [68], the increase of viscosity at high shear rates shown by Boersma et al. [69], the Brownian shear-thinning nature of suspensions characterized by Phung et al. [70], and the influence of particle roughness reported by Bousfield [71].

Particle level models show that structures of particles can form in shear fields. These structures can span the gap between the web and the blade. This mechanism is the same as those reported by Brady and Bossis [64] and by Boersma et al. [69]. When a cluster of particles forms in this geometry, large forces are transmitted between the web and the blade. This mechanism could be responsible for blade wear and blade deposits, if these structures exit the blade. Figure 9 depicts this situation: particles are forced closer together as the fast moving particles must past the slow moving particles near the blade. If the electrostatic or steric repulsive forces are not significant to keep the particles separated, particle clusters can span the gap between the blade and the web.

Particle level models have been able to predict that a viscoelastic behavior can exist in these systems. Toivakka et al [72] shows that electrostatic and steric forces keep the particles well separated, but when a strain occurs on the system, particles are

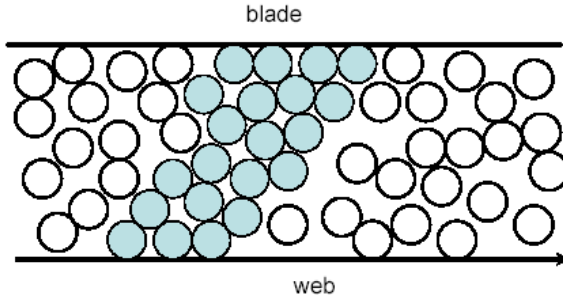


**Figure 9:** Schematic of the results from a particle motion model showing the clustering of pigments between the blade surface and the web at high shear rates.

forced closer together. This mechanism stores energy in the system to cause an elastic response. Example of this type of experimental system was reported by Fadat and Rigdahl [56] for coating suspensions. If the deformation is too large, particles move away from the static position and a non-linear viscoelastic result.

The influence of particle size distribution on coating rheology and flows has been predicted by particle level models. Chang and Powell [68] show how small particles can disrupt the formation of clusters and, thereby, reduce the shear viscosity. Toivakka and Eklund [67] confirm this mechanism and show how small particles can

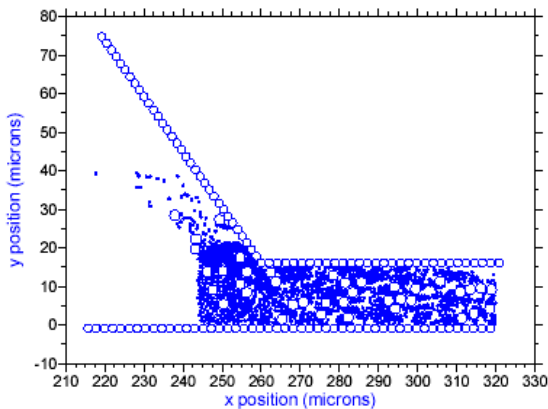


**Figure 10:** Particle configuration from Lyons et al. [73] for inlet particle size distribution. Top particles represent the blade surface and do not move. Bottom row of particles represent the paper web and move from left to right.

end up closer to the blade surface during shear. Fine particles are able to be closer to the solid boundaries because of their size. In addition, when particles are exposed to a flow field, larger particles must move faster than the finer particles near the walls. This velocity difference causes the larger particles to push the smaller particles even closer to the walls. After a number of interactions, the larger particles migrate away from the walls. This would create a separation of particles according to size, with the finer particles near the solid boundaries. The coating layer could have gradients of particles from its surface to the bulk. Lyons et al. [73] show that in the blade coating geometry, a separation of particle sizes can occur generating a layer of small particles near the blade surface; Figure 10 depicts the fine particle migration towards the blade surface. Bousfield et al. [74] show that the free surface after the blade may cause a similar separation of particles based on size, with the smaller particles being located at the top surface. These results may explain the high concentration of latex binder at the top layer of the coating observed industrially.

### 3.2. Models of Coating Flows

Initial attempts to model the blade coating operation are based on Newtonian fluids. For example, Turai [75], and others give simple analyses to relate shear rates, viscosity, geometry, and web velocity to the force generated on a blade during coating. Lubrication theory is used to reduce the complexity of the equations. The pressure distribution under the blade is found to be a strong function of the blade operating angle. Saita and Scriven [76] used lubrication theory to relate the details of the blade geometry or blade deflection to the coat weight and blade loading. Inertial forces of the fluid were found to be important in roll applicator systems [77].

Finite element methods were used by Pranckh and Scriven [78] and Vital et al. [79] to solve the two dimensional equations for the flow before, under and after the blade assuming a Newtonian fluid. The solution is in conjunction with a nonlinear beam equation that describes the deflection of the blade and a spring model that describes the deformation of the rubber backing roll and the web. Surface tension forces upstream from the blade and after the blade were included in the analysis. In the flow field, there is a stagnation line that separates the coating that is returned and the coating that is metered onto the web. The pressure distribution near the heel of the blade and under the blade tip shows little pressure gradients in the vertical direction: this result indicates that lubrication theory is valid in this region. Again, the operating angle of the blade is found to be a critical issue in these flows. The pressure distribution shows a stagnation pressure upstream of the blade, which is close to  $\frac{1}{2} \rho V^2$ , and a pressure increase near the blade heel due to viscous forces. This result links the pressure pulse due to the inertial terms with that of lubrication theory.

The influence of the absorption into the porous web on the flow field is modeled by Chen and Scriven [80]. The pressure distribution of a roll applicator and by a blade metering element from Pranckh and Scriven [78] is used to calculate the penetration depth of the coating. Bousfield [81] proposed a model to describe the formation of a filter cake on the web during blade coating. Lubrication theory was found to duplicate the pressure distribution of Pranckh and Scriven [78] and was used

to describe the dewatering and subsequent filter cake buildup on the paper web. The model by Bousfield [81] is shown to predict the onset of operational difficulties of literature data, if dewatering parameters are known. These difficulties seem to be related to the growth of a filter cake which had a thickness near the blade-paper gap.

The influence of the shear thinning nature of coating was described by Modrak [82]. A power-law model was used in conjunction with lubrication theory to describe the flow in a “rounded” blade. Viscosity data from a capillary viscometer was fitted for a Newtonian-like fluid, a shear-thinning coating, and a shear-thickening fluid. The power-law exponent varied from 0.675 to 1.3. The stagnation point moved downstream under the blade tip as the coating became shear thickening. The pressure distribution and the hydrodynamic lift on the blade were an order of magnitude higher for the shear thickening fluid, even though at a shear rate of  $3 \times 10^4 \text{ s}^{-1}$ , the shear viscosities were similar. However, the shear rate under the blade tip must reach  $10^6 \text{ s}^{-1}$ . For the three coatings, the shear-thinning model did a reasonable job at predicting pilot scale data.

Roper and Attal [55] and Isaksson et al. [83] used finite element techniques to calculate the flow field for viscous shear thinning fluids. Free surfaces and inertial terms were included in the later analyses. The coating was described as a power-law model with various values of the power-law index. The circulation within the pond of the short dwell coater was calculated to change from a single vortex at high viscosity values to two vortices at low viscosity values. The shear thinning nature of the fluid was found to reduce the pressure distribution under the blade and decrease the total blade loading. In addition, shear thinning fluids are found to produce a “plug flow” nature to the flow field, where most of the shear can occur in a thin layer near the moving web. The influence of blade angle and “slip” at the blade-coating interface are also discussed in Isaksson and Rigdahl [84].

Two-dimensional solutions for a viscoelastic fluid are described in Sullivan et al. [85], Olsson [86], and Olsson and Isaksson [87]. The results by Olsson use a geometry that closely resembles the blade geometry of paper coating. An upper convected Maxwell fluid, an Oldroyd-B fluid, and a Giesekus fluid are used as constitutive equations. The pressure distributions and streamlines are significantly

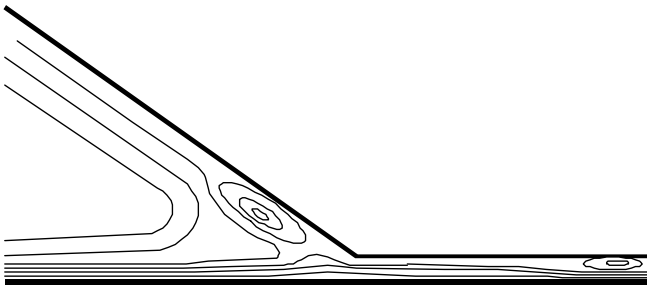


**Figure 11:** Streamlines for the flow of an Oldroyd –B fluid in a blade geometry. Blade is top boundary and web is lower boundary. From Olsson and Isaksson [87].

influenced by the presence of viscoelasticity. A recirculation region is predicted upstream from the blade tip and near the exit of the blade, as depicted in Figure 11. The pressure is predicted to decrease due to the extensional components of the flow field. This result would produce a lower blade force to obtain the same coat weight, as compared to a Newtonian fluid. The entrance region seems to be “clogged” with a vortex, resulting in less fluid that is able to pass under the blade. This result resembles the outcome of Sullivan et al. [85] where the force on the blade is reduced because of the influence of viscoelasticity.

The K-BKZ constitutive equation was used by Mitsoulis and Triantafillopoulos [88] to describe the flow under a blade with the influence of a free surface. The K-BKZ constitutive equation has multiple relaxation times and predicts normal forces. The pressure distributions and the net flow rate under the blade are influenced by the viscoelastic nature of the constitutive equation.

#### 4. CONCLUDING REMARKS

The rheology of a number of process streams are important to the paper industry. Pulp and coating suspensions are two examples that have some common features, but are also quite different. Pulp suspension flow is determined much by particle friction and fiber characteristics. An apparent yield stress is an important parameter in determining the flow behavior and the formation of flocs. Coating suspension rheology is determined by particle size distribution and particle interactions. For both types of suspensions, particle level models have helped increase our fundamental understanding of these microscopic mechanisms that influence the large scale behavior. In both cases, the depletion of particles or fibers from the wall can generate an apparent slip layer. This feature may be needed in future models to well describe the flow behavior.

#### ACKNOWLEDGEMENT

I thank my colleague Prof. Joseph Genco, for help with the early literature on pulp suspension flows.

#### REFERENCES

1. Nissan, A. H., Higgins, H. G. and Lagani, A., *The significance of rheology in the making and using of paper*, Trans. Soc. Rheol., 4 (1960) 207-232.
2. Casey, J. P., *Pulp and Paper, Chemistry and Chemical Technology*, Wiley, New York (1980).

3. Cui, H. and Grace, J. R., *Flow of pulp fibre suspension and slurries: A review*, Int. J. Multiphase Flow, 33 (2007) 921-934.
4. Moller, K., *General correlations of pipe friction data for pulp suspensions*, TAPPI J., 59(8) (1976) 111-114.
5. Duffy, G. G., *A review and evaluation of design methods for calculating friction loss in stock piping systems*, TAPPI J., 59 (1976) 124-127.
6. Moller, K. and Elmqvist, G., *Head losses in pipe bends and fittings*, TAPPI J., 63(3) (1980) 101-104.
7. Ogawa, K., Yoshikawa, S., Ikeda, J. and Ogawa, H., *Pressure loss and velocity profile of pulp flow in a circular pipe*, TAPPI J. 63 (1990) 217-221.
8. Hemstrom, G., Moller, K. and Norman, B., *Boundary layer studies in pulp suspension flow*, TAPPI J., 59(8) (1976) 115-118.
9. Laskey, H. L., *Optimum design of pulp stock pipelines*, TAPPI J., 61 (1988) 79-83.
10. Shelden, R. A., *Economic considerations in the pumping of pulp suspensions*, J. Pulp Paper Sci., 8(3) (1982) 49-52.
11. Kroeher, B., *Rheology of pulp suspensions*, Papier, 48(6) (1994) 298-308.
12. Gullichsen, J. and Harkonen, E., *Medium consistency technology I. Fundamental data*, TAPPI J., 64(6) (1981) 69-72.
13. Li, T. Q., Powell, R. L., Odberg, L., McCarthy, M. J. and McCarthy, K., *Velocity measurements of fiber suspensions in pipe flow by the nuclear magnetic resonance imaging method*, TAPPI J., 77(3) (1994) 145-149.
14. Hemstrom, G., Moller, K. and Norman, B., *Boundary layer studies in pulp suspension flow*, TAPPI J., 59(8) (1976) 115-118.
15. Ventura, C., Blanco, A., Negro, C., Ferreira, P., Garcia, F. and Rasteiro, M., *Modeling pulp fiber suspension rheology*, TAPPI J., 6(7) (2007) 17-23.
16. Bennington, C. P. J., Kerekes, R. J. and Grace, J. R., *The yield stress of fibre suspensions*, Can. J. Chem. Eng., 68 (1990) 748-757.
17. Bennington, C. P. J., Azevedo, G., John, D. A., Birt, S. M. and Wolgast, B. H., *The yield stress of medium and high consistency mechanical pulp fibre suspensions at high gas contents*, J. Pulp Paper Sci., 21 (1995) 111-118.
18. Kerekes, R. J., Soszynski, R. M. and Tam Doo, P.A., *The flocculation of pulp fibres*, Trans. Eight Fund. Res. Symp. [Ed: Punton, V.]. Mech. Eng. Publ. Ltd. Oxford, 1 (1985) 265-310.
19. Dalpke, B. and Kerekes, R.J., *The influence of pulp properties on the apparent yield stress of flocculated fibre suspensions*, Annual Meeting Preprints - Pulp and Paper Technical Association of Canada, 91st, Montreal, QC, Canada, (2005) 1-14.

20. Meyer, R. and Wahren, D., *On the elastic properties of three-dimensional fibre networks*, Sven. Papperstidn., 67 (1964) 432-436.
21. Paul, T., Duffy, G. and Chen, D., *New insights into the flow of pulp suspensions*, TAPPI J. Solutions, 1(1) (2001) 1-20.
22. Lee, P. F. W. and Duffy, G. G., *An analysis of the drag reducing regime of pulp suspension flow*, TAPPI J., 59(8) (1976) 119-122.
23. Soszynski, R. M. and Kerekes, R. J., *Elastic interlocking of nylon fibers suspended in liquid. Part 1. Nature of cohesion among fibers*, Nord. Pulp Pap. Res. J., 4 (1988) 172-179.
24. Roux, J. C., Franc, N., Duffy, G. G. and Fabry, B., *Shear factor: a new way to characterize fiber suspension shear*, TAPPI J., 84(8) (2001) 1-18.
25. Swerin, A., Powell, R. L. and Oedberg, L., *Linear and nonlinear dynamic viscoelasticity of pulp fiber suspensions*, Nordic Pulp Paper Res. J., 7(3) (1992) 126-32, 143.
26. Swerin, A., *Rheological properties of cellulosic fiber suspensions flocculated by cationic polyacrylamides*, Coll. Surf., A: Physicochem. Engng Asp., 133(3) (1998) 279-294.
27. Swerin, A., Risinger, G. and Oedberg, L., *Shear strength in papermaking suspensions flocculated by retention aid systems*, Nordic Pulp Paper Res. J., 11(1) (1996) 30-5.
28. Negro, C., Fuente, E., Blanco, A. and Tijero, J., *Effect of chemical flocculation mechanisms on rheology of fibre pulp suspensions*, Nordic Pulp Paper Res. J. 21(3) (2006) 336-341.
29. Martinez, D. M., Kiiskinen, H., Ahlman, A. K. and Kerekes, R. J. *On the mobility of flowing papermaking suspensions and its relationship to formation*, J. Pulp Paper Sci., 29(10) (2003) 341-347.
30. Batchelor, G. K., *Slender-body theory for particles of arbitrary cross-section in Stokes flow*, J. Fluid Mech., 44 (1970) 419-440.
31. Batchelor, G. K., *The stress system in a suspension of force-free particles*, J. Fluid Mech., 41 (1970) 545-570.
32. Claeys, I. L. and Brady, J. F. *Suspensions of prolate spheroids in Stokes flow. Part 1. Dynamics of a finite number of particles in an unbounded fluid*, J. Fluid Mech., 251 (1993) 411-442.
33. Claeys, I. L. and Brady, J. F., *Suspensions of prolate spheroids in Stokes flow Part 2. Statistically homogeneous dispersions*, J. Fluid Mech., 251 (1993) 443-477.
34. Yamane, Y., Kaneda, Y. and Doi, M., *Numerical simulation of semi-dilute suspensions of rodlike particles in shear flow*, J. Non-Newt. Fluid Mech., 54 (1994) 405-421.

35. Fan, X. J., Phan-Thien, N. and Zheng, R., *A direct simulation of fibre suspensions*, J. Non-Newt. Fluid Mech., 74 (1998) 113-135.
36. Harlen, O. G., Sundararajakumar, R. R. and Koch, D. L., *Numerical simulation of a sphere settling through a suspension of neutrally buoyant fibers*, J. Fluid Mech., 388 (1999) 355-388.
37. Sundararajakumar, R. R. and Koch, D. L., *Structure and properties of sheared fiber suspensions with mechanical contacts*, J. Non-Newtonian Fluid Mech., 73 (1997) 205-239.
38. Yamamoto, S. and Matsuoka, T., *A method for dynamic simulation of rigid and flexible fibers in a flow field*, J. Chem. Phys., 98 (1993) 644-650.
39. Ross, R. F. and Klingenberg, D. J., *Dynamic simulation of flexible fibers composed of linked rigid bodies*, J. Chem. Phys., 106 (1997) 2949-2960.
40. Schmid, C. F., Switzer, L. H. and Klingenberg, D. J., *Simulations of fiber flocculation: Effects of fiber properties and interfiber friction*, J. Rheol., 44 (2000) 781-809.
41. Switzer, L. H. and Klingenberg, D. J., *Rheology of sheared flexible fiber suspensions via fiber-level simulations*, J. Rheol., 47 (2003) 759-778.
42. Lindstrom, S. B. and Uesaka, T., *Simulation of the motion of flexible fibres in viscous fluid flow*, Phys. Fluids, 19 (2007) 113307.
43. Lindstrom, S. B. and Uesaka, T., *Simulation of semidilute suspensions of non-Brownian fibres in shear flow*, J. Chem. Phys., 128 (2008) 024901.
44. Olson, J. A., Frigaard, I., Chan, C. and Hamalainen, J. P., *Modeling a turbulent fibre suspension flowing in a planar contraction: The one-dimensional headbox*, Int. J. Multiphase Flow, 30 (2004) 51-66.
45. Green, S. I. and Kerekes, R. J., *Numerical analysis of pressure pulses induced by blades in gap formers*, TAPPI J., 81(4) (1998) 180-185.
46. Roshanzamir, A., Green, S. I. and Kerekes, R. J. *Two dimensional simulation of pressure pulses in blade gap formers*, J. Pulp Paper Sci., 24(11) (1998) 364-371.
47. Zahrai, S. and Bark, F.H., *On the fluid mechanics of twin wire blade forming in paper machines*, Nordic Pulp Paper Res. J., 4 (1995) 245-252.
48. Walters, J. C., *The Coating Processes*, TAPPI Press, Atlanta, GA, 1994.
49. Bousfield, D.W. and Co, A., *Paper coating rheology*, in *Advances in the flow and rheology of non-Newtonian fluids Part B*. [Eds: Siginer, K. and Chhabra. R. P.], Elsevier Science, NY, 1999, pp.827-842.
50. Van Gilder, R., Lee, D. I. and Purfeerst, R., *The effect of coating color solids on properties and surface uniformity*, TAPPI J., 66 (1983) 49-55.
51. Carreau, P. J. and Lavoie, P.-A., *Proc. 1993 TAPPI Advanced Coating Fundamentals Symp.*, TAPPI Press, Atlanta, GA (1993) 1.

52. Purkayastha, S. and Oja, M.E., *Proc. 1993 TAPPI Advanced Coating Fundamentals Symp.*, TAPPI Press, Atlanta, GA (1993) 31.
53. Ghosh T., *Proc. 1997 TAPPI Advanced Coating Fundamentals Symp.*, TAPPI Press, Atlanta, GA (1997) 43.
54. Barnes, H. A., Hutton, J. F. and Walters, K., *An Introduction to Rheology*, Elsevier Science, 1989.
55. Roper, J. A. and Attal, J., *Evaluations of coating high-speed runnability using pilot coater data, rheological measurements and computer modeling*, TAPPI J., 76(5) (1993) 55-61.
56. Nisogi, H., Bousfield, D. W. and Lepoutre, P., *Influence of coating rheology on final coating properties*, TAPPI J. 83(2) (2000) 100-106.
57. Windle, W. and Beazley, K. M., *The Mechanics of Blade Coating*, Tappi, 50(1) (1967) 1-7.
58. Triantafillopoulos, N., *Paper Coating Viscoelasticity and Its Significance in Blade Coating*, TAPPI Press, Atlanta, GA, 1996.
59. Fadat, G. and Rigdahl, M., *Viscoelastic properties of CMC/latex coating colors* Nordic Pulp Paper Res. J., 1 (1987) 30-38.
60. Kokko, A., Grankvist, T. and Triantafillopoulos, N., *Apparent slip velocity of paper coatings in viscometric flows*, Nordic Pulp Paper Res. J., 15(5) (2000) 502-508.
61. James, D. F., Yogachandran, N. and Roper, J. A. *Fluid elasticity in extension, measured by a new technique, correlates with misting*, Proc. 1993 Adv. Coating Fundam. Symp., (1993)
62. Ascaniol G., Carreau, P. J., Reglat, O. and Tanguy, P. A., *Extensional properties of coating colors at high strain rates*, Proc. 1993 Adv. Coating Fundam. Symp., (1993),
63. Kokko, A., *Evaluation of viscosity, elongational viscosity and dewatering of coating colors at high shear rates*, PhD Thesis, Åbo Akademi, Turku, Finland, (2001).
64. Brady, J. F. and Bossis, G., *The rheology of concentrated suspensions of spheres in simple shear flow by numerical simulations*, J. Fluid Mech. 155 (1985) 105-115.
65. Brady, J. F. and Bossis, G., *Stokesian Dynamics*, Ann. Rev. Fluid Mech., 20 (1988) 111-157.
66. Durlofsky L., Brady, J. F. and Bossis, G., *Dynamic simulation of hydrodynamically interacting particles*, J. Fluid Mech., 180 (1987) 21-49.
67. Toivakka, M. O. and Eklund, D. E., *Prediction of suspension rheology through particle motion simulation*, TAPPI J., 79 (1996) 211.
68. Chang, C. and Powell, R. L. *Effect of particle size distribution on the rheology of concentrated bimodal suspensions*, J. Rheol., 38 (1994) 85-98.

69. Boersma, W. H., Laven, J. and Stein, H. N., *Computer simulations of shear thickening of concentrated dispersions*, *J. Rheol.*, 39(5) (1995) 841-860.
70. Phung, T. N., Brady, J. F. and Bossis, G., *Stokesian dynamics simulation of brownian suspensions*, *J. Fluid Mech.* 315 (1996) 345-365.
71. Bousfield, D. W., *Particle Motion During Shear: The Influence of Particle Shape and Roughness on Rheology*, *Nordic Pulp Paper Res. J.*, 8 (1993)176-183.
72. Toivakka, M., Eklund, D. and Bousfield, D. W., *Prediction of Suspension Viscoelasticity Through Particle Motion Modeling* *J. Non-Newt. Fluid Mech.*, 56 (1995) 49-64.
73. Lyons, A., Iyer, R. and Bousfield, D. W., *Particle motion modeling of particle size distributions in blade geometries*, *Proc. 2003 Adv. Coating Fundam. Symp.* (2003) pp. 254-263.
74. Bousfield, D. W., Isaksson, P. and Rigdahl, M., *Modeling of Particle Motion at the Exit of a Blade Coater*, *J. Pulp Paper Sci.* 23(6) (1997) J293-J297.
75. Turai, L. L., *Analysis of the Blade Coating Process*, *TAPPI J.*, 54(8) (1971) 1315-1318.
76. Saita, F. A., and Scriven, L. E., *Coating flow analysis and the physics of flexible blade coating*, *Proc. TAPPI Coating Conf.*, TAPPI Press, Atlanta, GA (1985) p. 13.
77. Eklund, D. and Kahila, S. J., *Processes occurring under the blade during blade coating*, *Wochbl. Papierfabr.*, 106 (1978) 661-665.
78. Pranchk, F. R. and Scriven, L. E. *The physics of blade coating of a deformable substrate*, *TAPPI J.*, 73 (1990) 163.
79. Vidal D. J., Bertrand, F. and Tanguy, P. A., *Numerical simulation of the hydrodynamics in a short-dwell coater*, *Chem. Eng. Sci.*, 53(11) (1998) 1991-2003.
80. Chen, K. S. A. and Scriven, L. E., *Liquid penetration into a deformable porous substrate*, *TAPPI J.*, 73(1) (1990) 151-161.
81. Bousfield, D. W., *Prediction of Velocity and Coat Weight Limits Based on Filtercake Formation*, *TAPPI J.*, 77(7) (1994) 161-171.
82. Modrak, J. P., *Effect of coating color rheology on the blade coating process*, *TAPPI J.*, 56 (1973) 70-76.
83. Isaksson, P., Engström, G., Rigdahl, M., *Experimental analysis of the dynamic equilibrium in the vicinity of the blade tip during blade coating*, *Nordic Pulp Paper Res. J.*, 3 (1994) 150-155.
84. Isaksson, P. and Rigdahl, M., *Numerical simulation of blade coating with short dwell and roll application coaters*, *Rheol. Acta*, 33 (1994) 454-467.
85. Sullivan, T., Middleman, S. and Keunings, R., *Use of a finite-element method to interpret rheological effects in blade coating*, *AIChE J.*, 33(12) (1987) 2047-2056.

86. Olsson, F. *A solver for time dependent viscoelastic fluid flow*, J. Non-Newtonian Fluid Mech., 51 (1994) 309-340.
87. Olsson, F. and Isaksson, P., *The influence of viscoelastic rheology on blade coating as revealed by numerical methods*, Nordic Pulp Paper Res. J., 10 (1995) 234-244.
88. Mitsoulis, E. and Triantafillopoulos, N., *Viscoelasticity in Blade Coating of Non-Newtonian Fluids*, TAPPI Adv. Coat. Fund. Symp., 1997.